TJNAF Proposal to PAC23

A Search for Evidence of Soft–Hard Factorization in Charged Pion Electroproduction

R. Ent, H. Fenker, D. Gaskell (spokesperson), M. Jones,
D. Mack (co–spokesperson), J. Roche, G. Smith, G. Warren, S. Wood
Jefferson Laboratory, Newport News VA 23606

J. Volmer
DESY Zeuthen, 15738 Zeuthen, Germany

J. Reinhold
Florida International University, Miami, FL 33199

E. Christy, C. Keppel, L. Tang
Hampton University, Hampton VA 23668

A. Agalaryan, R. Asaturyan,
H. Mkrtchyan, S. Stepanyan, V. Tadevosyan
Yerevan Physics Institute, Armenia

Contents

Abstract

We propose a search for evidence of soft–hard factorization for $Q^2 \leq 4$ in exclusive electroproduction of charged pions on the nucleon. A separation of the longitudinal and transverse cross sections will be made at fixed $x_B = 0.5$ and $-t = 0.38$. The primary goal is to determine the Q^2 dependence of the longitudinal cross section with errors small enough to test whether the data have, or are evolving toward, the predicted Q^{-6} dependence. The secondary goal is to determine whether the L/T ratio in π^- electroproduction on the neutron is so large that the longitudinal cross section can be extracted from unseparated, high ϵ measurements without an explicit L–T separation, a feature which would greatly facilitate measurements of $n(e, e'\pi^-)p$ with large acceptance instruments like the CLAS. If soft–hard factorization is valid, these measurements will be sensitive to the two polarized GPD's, $\widetilde{H}_q$ and $\widetilde{E}_q$. Thus, our proposed experiment complements measurements of not only DVCS, which is a function of all 4 GPD's, but also vector meson electroproduction, which is a function of the unpolarized GPD's, H_q and E_q. This complementarity is critical because, while it may be possible to construct ansatzes for all the GPD's which are consistent with present or future DVCS data, a GPD program without meson electroproduction input will be very limited simply because the photon is blind to quark flavor. Our proposed experiment will provide a first precision measurement of separated charged pion cross sections at $Q^2 = 3$ to 4 GeV^2 and will play an essential role in guiding future GPD programs.

1 Introduction

1.1 Soft–Hard Factorization and GPD's

"Soft–hard factorization" refers to the factorization of meson electroproduction into a hard component, corresponding to the virtual photon coupling to a quark and its development into a meson, and a "soft" component corresponding to the probability of removing a quark with a given flavor and momentum fraction and replacing it with a quark of a different momentum fraction and/or flavor [1] (see Figure 1). The soft component can be described using Generalized Parton Distributions (GPD's), while the hard component is calculable. The soft–hard factorization theorem for meson electroproduction applies only to longitudinal photons. Thus, strictly speaking, the only observables to which it applies are the longitudinal cross section and the transverse target Single Spin Asymmetry.

While it is often claimed that contributions from the transverse cross section should be suppressed by a factor of $1/Q^2$, the Q^2 at which this might be true is undetermined at the present time [2]. Precocious factorization, in which higher order effects may cancel in the ratios of unseparated observables ($\sigma_{\pi^+}/\sigma_{\pi^0}$, for example) is therefore unlikely unless the longitudinal response in both the numerator and denominator is dominant. Even if precocious factorization were observed, one would immediately wish to know the relative longitudinal and transverse contributions. The interpretation of ongoing or future ratio measurements would strongly benefit from a larger database of L–T separated cross sections.

There is optimism that DVCS measurements will be consistent with soft–hard factorization at modest Q^2 and that this will give access to the GPD's. The reason for this optimism is the close relationship of DVCS to DIS, which is known to behave perturbatively at relatively modest Q^2. However, since DVCS is a function of all 4 GPD's (E_q, H_q, $\widetilde{E_q}$, and $\widetilde{H_q}$), only 2–3 of which may dominate in a given kinematics [3], it would be a challenge to test ansatzes for all 4 GPD's using DVCS alone, and impossible to test the quark flavor dependence of the GPD's. A successful GPD program will require data from the meson electroproduction sectors.

While DVCS is a function of 4 quark flavor-dependent GPD's, longitudinal meson electroproduction is superficially less complex: electroproduction of vector mesons like the ρ depends only on E_q and H_q, while electroproduction of pseudoscalar mesons like the π depends only on $\widetilde{E_q}$ and $\widetilde{H_q}$. The H_q and $\widetilde{H_q}$ terms normally dominate DVCS since the E_q and $\widetilde{E_q}$ terms are kinematically suppressed. In general, the H_q and $\widetilde{H_q}$ contributions are also important in meson electroproduction. However, in the case of charged pion electroproduction, the presence of a strong t-channel pole

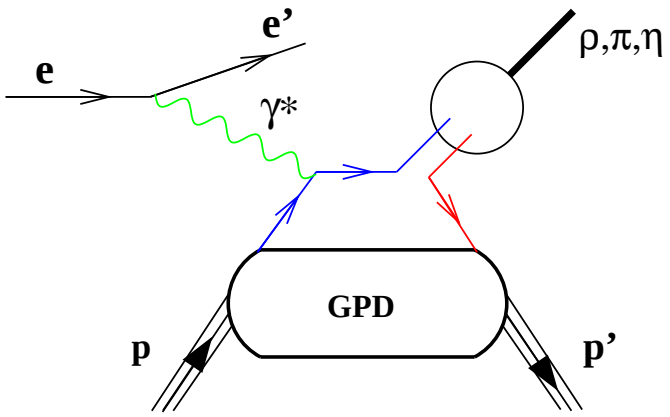

Figure 1: Handbag diagram describing hard, exclusive meson electroproduction. In this picture, the process can be factorized into a soft component which describes the probability to remove a parton of a certain momentum and flavor and replace a parton with a different momentum and/or flavor, and a hard component which describes the virtual photon coupling to the quark and the subsequent creation of a meson. The soft component can be parameterized in terms of Generalized Parton Distributions while the hard component is calculable.

makes $\widetilde{E_q}$ overwhelmingly dominant at low $-t$. For π^+ or π^- production, it is quite difficult to raise $-t$ large enough to make $\widetilde{E_q}$ and $\widetilde{H_q}$ comparable without violating the Collins condition that $-t$ should be much less than Q^2. At the $-t$ proposed here ($-t \approx 0.38$ GeV^2), the two terms are expected to be of comparable magnitude (see also Figure 2), hence our proposed measurement offers new information which is unattainable from the existing very low $-t$ data from the pion charge form factor experiment, E93-021 [4].[1]

1.2 Testing soft–hard factorization

Before anything can be learned about GPD's from meson electroproduction, we must determine whether soft–hard factorization applies in our kinematic regime. There is no single test that will prove this. We must therefore explore every necessary condition for factorization and build a case (albeit a circumstantial one) that we have indeed reached Q^2 values where it applies. Perhaps the most stringent test is

[1] The E93-021 measurements were also at fixed W rather than fixed x_B.

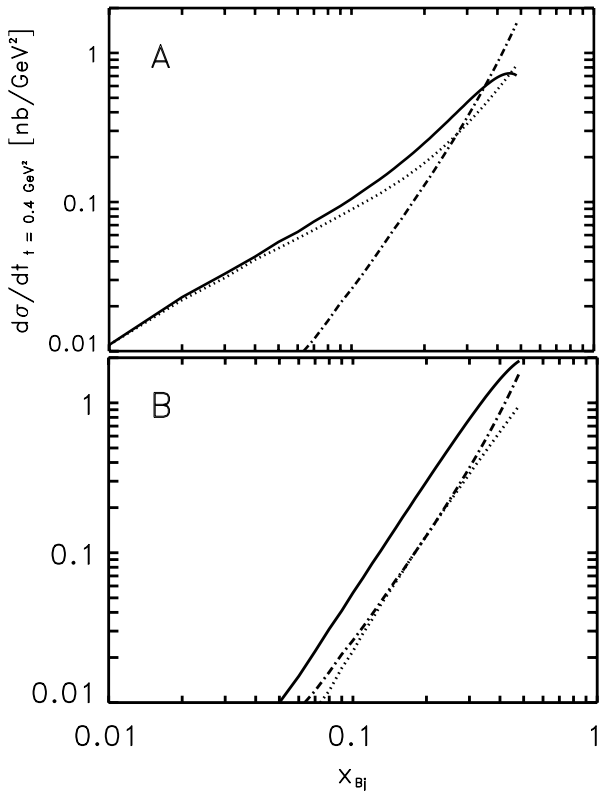

Figure 2: Cross section for exclusive π^+ production at constant $-t = 0.4$ GeV^2 and $Q^2 = 10$ GeV^2 for two models from Ref. [5]. The solid line is the full calculation, the dot–dashed line is the contribution from the pion pole–like piece (which dominates the contribution from $\widetilde{E_q}$), and the dotted line is the contribution from the non–pole piece, $\widetilde{H_q}$. The models A (top) and B (bottom) differ only in the way in which they treat the t dependence of the parton distributions that contribute to the non–pole piece. At $x_B = 0.5$, the pole–like term is only about a factor of three larger than the non–pole term indicating that the $\widetilde{H_q}$ term is not overwhelmed by the $\widetilde{E_q}$ contribution. Note that although Q^2 is rather large in this calculation, the more relevant degree of freedom for assessing the relative importance of the pole contribution is $-t$.

to see if the longitudinal cross section has the predicted dependence on Q^2[1] (at fixed x_B and $-t$),

$$\frac{d\sigma_L}{dt} \propto \frac{1}{Q^6}.$$

If this test is passed, then one can try to gather further evidence such as comparing the measured magnitude (as opposed to just the Q^2 dependence) of the longitudinal cross sections to the predictions of several reasonable GPD ansatzes. Indeed, in the case of an apparent $1/Q^6$ dependence, one may in turn look at the longitudinal cross sections as further constraining GPD models.

The prediction for the L/T ratio

$$\frac{d\sigma_L}{dt}/\frac{d\sigma_T}{dt} \propto Q^2$$

is a somewhat weaker test since there are several ways to get this behavior that do not require soft–hard factorization. In addition, the Q^2 dependence of the transverse cross section is quite uncertain even in the perturbative limit due to endpoint contributions (at finite Q^2). Nevertheless, we will be able to perform this test as well.

Our proposed measurement on charged, pseudoscalar mesons, is a logical complement to the completed Hall B experiment E99-105, "Deeply Virtual Electroproduction of Vector Mesons", which uses the assumption of s–channel helicity conservation to relate the decay angular distribution of ρ mesons to σ_L and σ_T. Indeed, such a complementary study of pseudoscalar meson production was also proposed in Hall B (PR99–106). In principle, a large acceptance detector like CLAS is the best device for measuring pseudoscalar meson electroproduction over a large range of $-t$ and x_B; as we will show, longitudinal–transverse separations using small solid angle spectrometers force $-t$ and x_B to be highly correlated. However, measurements with focusing spectrometers benefit from relatively small point–to–point systematic errors which are needed for L–T separations. In Hall C, previous charged pion electroproduction experiments (E91003 and E93021) have achieved point–to–point uncorrelated errors of 2–2.4% [6, 7]. With modest changes to the experimental configuration which will decrease uncertainties in the spectrometer acceptance, point–to–point uncorrelated errors of 2% are achievable.

Unlike most of the meson electroproduction channels under discussion for GPD's, charged pion electroproduction is accessible (at high luminosity) to a pair of relatively small solid angle, focusing magnetic spectrometers. The Rosenbluth technique permits an unambiguous isolation of the longitudinal cross section. Hall C acquired

significant experience doing L–T separations with charged pions during the successful F_π (E93021) and NucPi (E91003) experiments. By fixing x_B, isolating the longitudinal response, and keeping $-t$ small relative to Q^2, we have tried to design an experiment consistent with the derivation of soft–hard factorization by Collins *et al.* [1].

It is not necessarily obvious that it is possible to fix $-t$ and x_B while varying Q^2, but we have demonstrated this numerically. Figure 3 shows the phase space in $-t$ vs x_B which is accessible to experiment (although derived for pion electroproduction, very similar plots could be constructed for ρ electroproduction or DVCS). The forbidden and accessible regions are separated by a locus of points which corresponds to parallel kinematics. There is a strong correlation between $-t_{min}$ and x_B which is nearly independent of modest variations in Q^2. Thus, although small solid angle, focusing magnetic spectrometers may be better at performing L–T separations, they are limited to measurements near $-t_{min}$. Above the locus (*i.e.* above $-t_{min}$) lies the region which is in principle accessible to large acceptance detectors like the CLAS provided the longitudinal response can be isolated.

This measurement will also have bearing on the future 12 GeV program at Jefferson Lab. Clearly, one will want to use a large acceptance device like CLAS to map out the x_B, $-t$, and Q^2 dependence of various processes to constrain GPD models as thoroughly as possible (without the correlation in $-t$ vs x_B found in parallel kinematics). However, the maximum Q^2 accessible in meson electroproduction reactions at 12 GeV in CLAS is about 8 GeV^2 for unseparated cross sections (as in ρ electroproduction where s-channel helicity conservation is assumed) and approximately 6 GeV^2 [8] for separated cross sections (as in $\pi^\pm$ electroproduction where an L–T separation must be performed). The latter Q^2 is not far above the maximum $Q^2 = 4$ GeV^2 of this proposal. Thus we are today in the position of being able to determine, at roughly the same Q^2 as where most of the 12 GeV CLAS charged pion electroproduction program may be carried out, whether one observes soft–hard factorization or whether higher order effects are still causing significant deviations from soft–hard factorization.

1.3 Theoretical Interpretability

The factorization theorem for hard exclusive electroproduction of mesons (and photons) states that the amplitude can be written,

$$A = \sum_{i,j} \int_0^1 \int dx_1 f_{i/p}(x_1, x_1 - x_B; t, \mu) H_{ij}(Q^2 x_1/x_B, Q^2, z, \mu) \phi_j(z, \mu) + ...$$

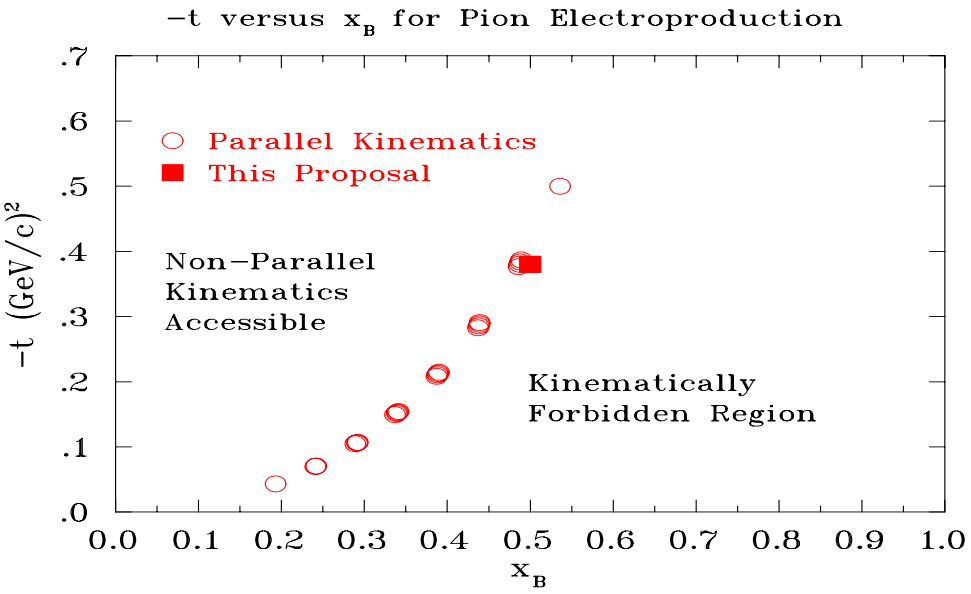

Figure 3: This figure shows the phase space in $-t$ vs x_B which is accessible to experiment. The locus of open circles corresponds to parallel kinematics and shows a strong correlation between $-t$ and x_B. The solid square marks the chosen kinematics of this proposal. Above the locus (*i.e.* above $-t_{min}$) lies the region which is accessible to large acceptance detectors like the CLAS.

where $f_{i/p}$ is a generalized parton distribution, ϕ_j is the distribution amplitude of the produced meson, and H_{ij} is a hard–scattering term calculable in QCD perturbation theory [9].

Higher order terms in the hard–scattering coefficient, H_{ij}, may mask the anticipated $1/Q^6$ behavior of the longitudinal charged pion cross section. Indeed, many theorists indicate that the corrections are likely sizable at values of Q^2 less than 10 GeV^2 [3, 10, 11]. Even at $Q^2 = 10$ GeV^2, calculations indicate that higher order corrections may still be significant (see Fig. 4).

Much hope for experimental access to GPD's relies on so–called precocious factorization, in which these higher order corrections to the hard–scattering coefficient cancel in asymmetries or ratios of observables. This may give experimental access to GPD's at lower Q^2's (≈2–4 GeV^2). However, observation of the leading order Q^2 dependence in asymmetries or ratios, while certainly suggestive of a cancellation of higher order effects, is not necessarily a very stringent test of factorization itself.

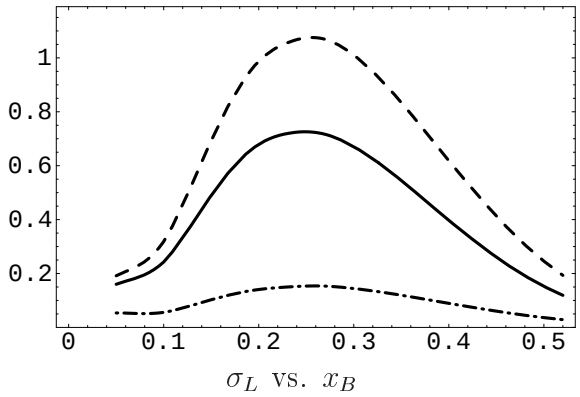

Figure 4: Longitudinal pion electroproduction cross section at $Q^2 = 10$ GeV^2 and $-t = -t_{min}$ [11]. The solid line denotes the leading order contribution while the dashed and dot–dashed lines are two models of the LO+NLO cross section. Even at this large Q^2, the NLO corrections are apparently quite large.

One needs a stricter test in which higher order effects are more likely to be apparent, *i.e.*, absolute (longitudinal) cross section measurements. If calculations that indicate cancellation of higher order terms in asymmetries and ratios also describe the Q^2 dependence of these cross sections, one then gains confidence that we really understand the mechanism by which precocious factorization comes about.

In summary, some may argue it is unlikely that one may see the predicted $1/Q^6$ dependence in longitudinal π^+ cross sections at the Q^2's proposed here. However, at the very least the data will serve as a rigorous constraint on any model that attempts to prove that precocious factorization in other observables, if it is observed, truly does result from the cancellation of higher order terms.

2 The Experiment

This experiment will measure separated cross sections for the $p(e, e'\pi^+)n$ and $n(e, e'\pi^-)p$ processes. The primary aim will be to measure the Q^2 dependence of the longitudinal π^+ proton cross section to $\approx 10\%$ to look for the onset of soft–hard factorization. The secondary goal will be to measure σ_T/σ_L for π^- production from the neutron to investigate whether the transverse cross section is so suppressed that future measurements can safely extract the longitudinal response from unseparated cross sections (as is done with the F_2 structure function in DIS). At the maximum

Q^2 of the F_π experiment (≈ 1.6 GeV^2), the ratio of transverse to longitudinal cross sections is about 0.25 [12]. Furthermore, Regge calculations (the VGL model of Vanderhaeghen, Guidal and Laget [13]), which roughly agree with the F_π data, predict that σ_T/σ_L continues to decrease with increasing Q^2. One should be cautious about applying the VGL model in a Q^2 range for which there is little π^- data, but we feel that the possibility of a very small transverse to longitudinal ratio is worth exploring.

Confirmation of this suppression would open the door for further studies with a large acceptance device like CLAS, where L–T separations are challenging. Since the transverse cross section is expected to be quite small, we should be able to measure σ_T/σ_L to an absolute precision of about ± 0.1 relatively easily.

The cross section for pion electroproduction can be written,

$$\frac{d\sigma}{dEd\Omega_e d\Omega_\pi} = \Gamma_V \mathcal{J} \frac{d\sigma}{dtd\phi},$$

where Γ_V is the virtual photon flux factor, t is the usual Mandelstam variable ($= (p_\pi - q)^2$) and ϕ is the azimuthal angle of the pion reaction plane relative to the electron scattering plane. The Jacobian, $\mathcal{J}$, is the transformation from $\cos\theta$ (where θ is the angle between the outgoing pion and the virtual photon direction) to t. $d\sigma/dtd\phi$ is the virtual photon cross section and can be written,

$$2\pi\frac{d\sigma}{dtd\phi} = \frac{d\sigma_T}{dt} + \epsilon\frac{d\sigma_L}{dt} + \sqrt{2\epsilon(\epsilon+1)}\frac{d\sigma_{LT}}{dt}\cos\phi + \epsilon\frac{d\sigma_{TT}}{dt}\cos 2\phi.$$

The interference terms (σ_{TT} and σ_{LT}) can be eliminated by averaging over ϕ and the longitudinal and transverse cross sections can be separated by measuring the cross section at two or more values of ϵ and fitting a line.

This experiment will measure the unseparated cross section at two values of ϵ for each of three values of Q^2, allowing the extraction of the separated longitudinal and transverse cross sections for π^+ production from the proton. The equivalent π^- cross sections from the neutron will be extracted by taking both π^+ and π^- data from the deuteron. The π^- cross section will then be extracted via,

$$\sigma_n^{\pi^-} = \sigma_D^{\pi^-}\frac{\sigma_p^{\pi^+}}{\sigma_D^{\pi^+}}.$$

The π^+ data on the deuteron is necessary to cancel possible wave function effects.[2]

[2]At the large values of $-t$ planned for this experiment, the most obvious nuclear effect, Pauli

Table 1: Basic parameters of the proposed experiment.

Pion Arm	HMS
PID	aerogel (π^+), gas Cer., Pb–glass (π^-)
Electron Arm	SOS
PID	Pb–glass, gas Cer.
Target	3cm LH_2, LD_2
Beam	75 μA,

The experiment will use standard Hall C equipment: the High Momentum Spectrometer (HMS) as the pion arm, the Short Orbit Spectrometer (SOS) for the electron arm, and the Hall C cryotarget. The basic setup is summarized in Table 1.

2.1 Kinematic Settings

In the factorization test proposed here, the Q^2 dependence of the longitudinal cross section will be examined at fixed $x_B = Q^2/(2M\nu)$ and fixed, relatively large, $-t$. The data will be taken in near-parallel kinematics, so that the separation of the response functions can be made.

An overview of the kinematics is shown in Table 2. As shown in Figure 5, there are many solutions that allow one to sample a relatively large range of Q^2 at constant x_B while staying above the resonance region. We have chosen the option that allows us to reach the largest possible Q^2. Figure 3 shows that this value of x_B corresponds to a value of $-t$ (0.38) which is small enough to be a good test of factorization, but large enough that the pion pole-like GPD, $\widetilde{E}$, is not overwhelmingly dominant.

2.2 Kinematic Calibrations and Acceptance Checks with $p(e, e'p)$

This experiment will require that the SOS be at large angles (up to 65 degrees). The y–target acceptance is fairly flat out to about $\pm$1.4 cm, dropping quickly beyond 1.6 cm. At 65 degrees, the effective length (as seen by the SOS) of a 4 cm target is

blocking, should not play a role. However, the missing–mass cut at 2–pion threshold will necessarily cut away some fraction of the deuteron wave function. Rather than estimate the fraction lost by this cut and correct for it in the extraction of the π^- cross section, it is simpler and more reliable to just measure the π^+ deuterium yield.

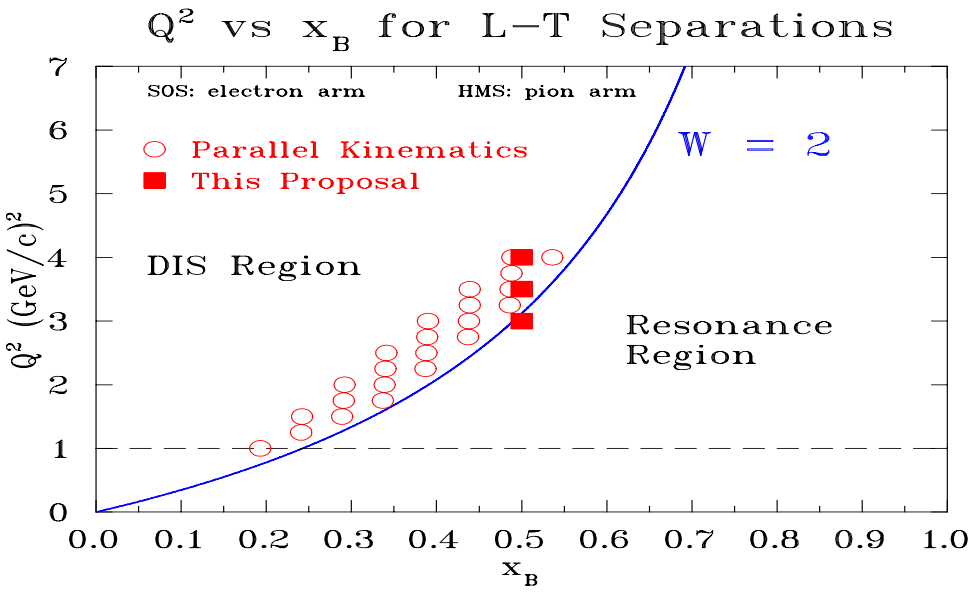

Figure 5: Q^2 vs. x_B phase space available for L–T separations in Hall C. There is a range of x_B for which one can measure a relatively large range of Q^2. We have chosen $x_B = 0.5$ to be able to measure the highest possible Q^2 (4 GeV^2) while maintaining a decent lever–arm with which to measure the Q^2 dependence of the longitudinal cross section.

about 3.6 cm, well beyond the onset of the region of rapid acceptance change. For this reason we plan to use a 3 cm cryotarget and ensure that the effective target length seen by the SOS is as consistent as possible at each setting. Nevertheless, we plan to confirm our understanding of the SOS acceptance at large angles using the well known elastic cross section.

We will also use elastic scattering to confirm our understanding of saturation effects in the SOS. At large central momenta (> 1.5 GeV/c), the effective central momentum of the SOS can deviate from the set value (which assumes a linear $B \propto I$ relationship) by as much as 0.8%. While this effect has been probed previously, we will use the over–constrained $p(e,e'p)$ process to make further studies and more fully map out this deviation as well as other higher order saturation effects in the SOS optics.

We plan to take about two shifts of hydrogen elastic data for these acceptance and kinematics studies.

Table 2: Kinematics for the proposed HMS-SOS measurement with $x_B = 0.5$ and $-t_{min} = .38$. An L-T separation is assumed and the ϵ range is given. The SOS is located at $\theta_{e'}$. The HMS minimum angle is 10.5 degrees, so at some settings the HMS angle is not identical to θ_{pq}.

Setting	Q^2	W	E_e (GeV)	E'_e (GeV)	θ'_E (deg)	P_π (GeV/c)	θ_{pq} (deg)	θ_{HMS} (deg)	ϵ
1a	3.0	1.97	4.960	1.763	34.06	2.995	15.75	15.75	0.547
1b			3.977	0.780	58.92		10.58	10.58	0.262
									$\Delta\epsilon$=0.29
2a	3.5	2.09	5.490	1.760	35.03	3.524	14.01	14.01	0.502
2b			4.690	0.960	52.32		10.49	10.50	0.294
									$\Delta\epsilon$=0.21
3a	4.0	2.21	6.0	1.737	36.09	4.053	12.55	12.55	0.459
3b			5.340	1.077	49.29		9.98	10.50	0.300
									$\Delta\epsilon$=0.16

2.3 Count Rate Estimates

The VGL Regge model [13] provides an overall good description of $N(e, e'\pi^{\pm})N$ for available low Q^2 data over an impressively large range of $-t$. Accordingly, we use it to make our rate and error estimates. However, it is not a microscopic model for hard $\gamma_v + q$ scattering processes and the predicted cross sections have a less steep fall-off at low Q^2 than the $1/Q^6$ dependence which is expected in the case of soft–hard factorization. However, the monopole ansatz for the Q^2 dependence in the VGL Regge model (fitted to the pion radius in the $Q^2 = 0$ limit) evolves to the hard scattering limit very rapidly. By $Q^2 = 3$, the predicted behavior at fixed x_B is nearly indistinguishable from $1/Q^6$. Thus, there is little likelihood that our cross sections are grossly overpredicted and that we won't be able to achieve our statistics goal. It is more likely that we will meet or exceed our statistics goals.

The longitudinal cross sections predicted by the VGL Regge model are given in Figure 6 and the estimated counting rates are shown in Tables 3 and 4. These rates assume π^+ (π^+ and π^-) production from 3 cm liquid hydrogen (deuterium) targets and 75 μA beam. Due to the increased ϵ range (and hence the reduced error amplification) we plan to only accumulate half as many events at the lowest Q^2

point (5,000 as opposed to 10,000).

Note that these estimates include cuts to match the kinematic phase space at high and low ϵ. At high ϵ one generally accepts a larger region of Q^2 and W than at low ϵ. Hence, to reduce systematic uncertainties, it is helpful to match the Q^2 and W coverage at both settings via software cuts.

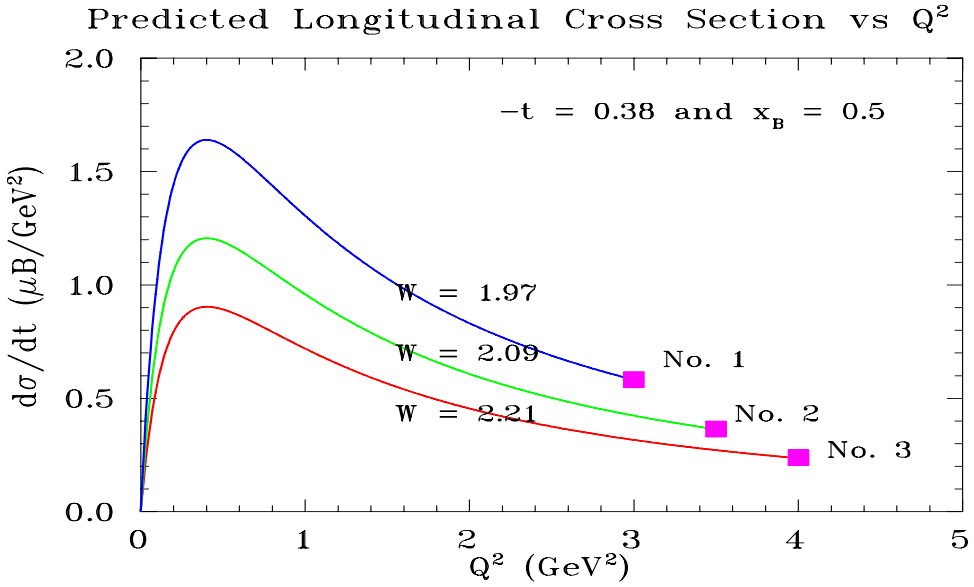

Figure 6: VGL Regge model longitudinal cross section versus Q^2 for loci of constant W. The proposed kinematic settings are solid squares at $-t_{min}$ labeled by number. Both $-t$ and x_B are fixed. The fixed x_B constraint in our kinematic settings causes the cross sections to drop rapidly with Q^2.

Another factor that comes into play is the acceptance in the angle between the produced pion and the virtual photon, θ_{pq}.[3] We restrict the coverage in θ_{pq} such that we have 2π coverage in ϕ_{pq} (the azimuthal angle between the hadron production plane and the scattering plane) for all θ_{pq}. This will reduce our sensitivity to the LT and TT interference terms which depend on ϕ_{pq}. Previous Hall C experiments have shown that when one has complete ϕ_{pq} coverage, one is rather insensitive to the precision of the determination of σ_{LT} and σ_{TT} [14]. The simulated θ_{pq} and ϕ_{pq}

[3] At fixed Q^2 and W, θ_{pq} also determines $-t$. We discuss θ_{pq} here because it is a bit easier to make the connection with spectrometer acceptance issues.

Table 3: Real $p(e,e'\pi^+)n$ coincidence rates after cuts to match the acceptances at the low and high ϵ settings. The rates are from a SIMC simulation which incorporates the following: VGL Regge model cross sections, pion decay, and radiative corrections. Rates are additionally corrected for anticipated detection efficiencies and pion absorption effects (about 10% taken all together).

Setting	Q^2 (GeV^2)	$d\sigma/dt$ (μb/GeV^2)	Rate Counts/Hour	Number of Events	Beam Hours
1a	3.0	0.52	356	5,000	14
1b		0.35	114	"	44
2a	3.5	0.29	307	10,000	33
2b		0.21	127	"	79
3a	4.0	0.17	179	"	56
3b		0.13	84	"	119
Total					345

Table 4: Real $D(e,e'\pi^+)nn$ and $D(e,e'\pi^-)pp$ coincidence rates after cuts to match the acceptances at the low and high ϵ settings. For the π^- rates, we have assumed that the ratio of longitudinal to transverse cross sections, $R = \sigma_L/\sigma_T$, is 10.

Setting	Q^2 (GeV^2)	π^+ Rate Counts/Hour	Hours per 500 π^+ events	π^- Rate Counts/Hour	Hours per 500 π^- events
1a	3.0	279	1.8	202	2.5
1b		90	5.5	54	9.5
2a	3.5	241	2.1	176	2.9
2b		102	4.9	64	7.5
3a	4.0	141	3.6	103	4.9
3b		66	7.5	44	11.4
Total			25.4		38.7

coverage for the $Q^2 = 3$ GeV^2 and the $Q^2 = 4$ GeV^2 kinematic points is shown in Figure 7. Note that at the $Q^2 = 4$ GeV^2, low ϵ setting, the HMS angle is not centered on the direction of $\mathbf{q}$, hence the θ_{pq} vs. ϕ_{pq} distribution appears somewhat off–center.

2.4 Backgrounds

2.4.1 Particle Identification

Strictly speaking, hadron identification in the HMS is not really necessary since "in–time" protons and kaons can be cleanly eradicated via coincidence time cuts, and those that remain will be only random coincidences which will be subtracted away. Nonetheless, to improve the real–to–random signal, it is desirable to have some kind of discrimination between pions and protons for the π^+ data, and between pions and electrons for the π^- data.

At the large pion momenta sampled in this experiment, time–of–flight will be inadequate to separate π^+'s and protons. This experiment will make use of the aerogel detector that has been built for experiment E00-108 ("Duality in Meson Electroproduction" – scheduled to run in the summer of 2003). This aerogel will have an index of refraction of 1.015, which will cleanly separate pions and protons at all our kinematic settings. When the HMS is used to detect π^-'s, we will use the standard HMS lead–glass calorimeter. At our kinematics, the π^-/e ratio in the HMS will always be significantly larger than 1.0, so the $> 99\%$ electron efficiency of the HMS calorimeter will be more than adequate.

Another consideration in this experiment is contamination from muons resulting from pion decay. At the lowest pion momentum, about 16% of the pions will decay in flight. Previous experience during the pion form–factor experiment has shown that a large fraction of the resulting muons do not make it to the detector focal plane (due to properties of the HMS optics). Muons (the correction for those that result in lost triggers and those that contaminate the pion spectra) are taken into account in the Hall C Monte Carlo, SIMC. The modeling of this process is reliable and contributes little uncertainty to the extraction of the experimental cross sections [6].

2.4.2 Accidental Coincidences

The singles rates in both the HMS and SOS have been estimated and are shown in Table 5. In the SOS, electron rates are estimated using the QFS program of

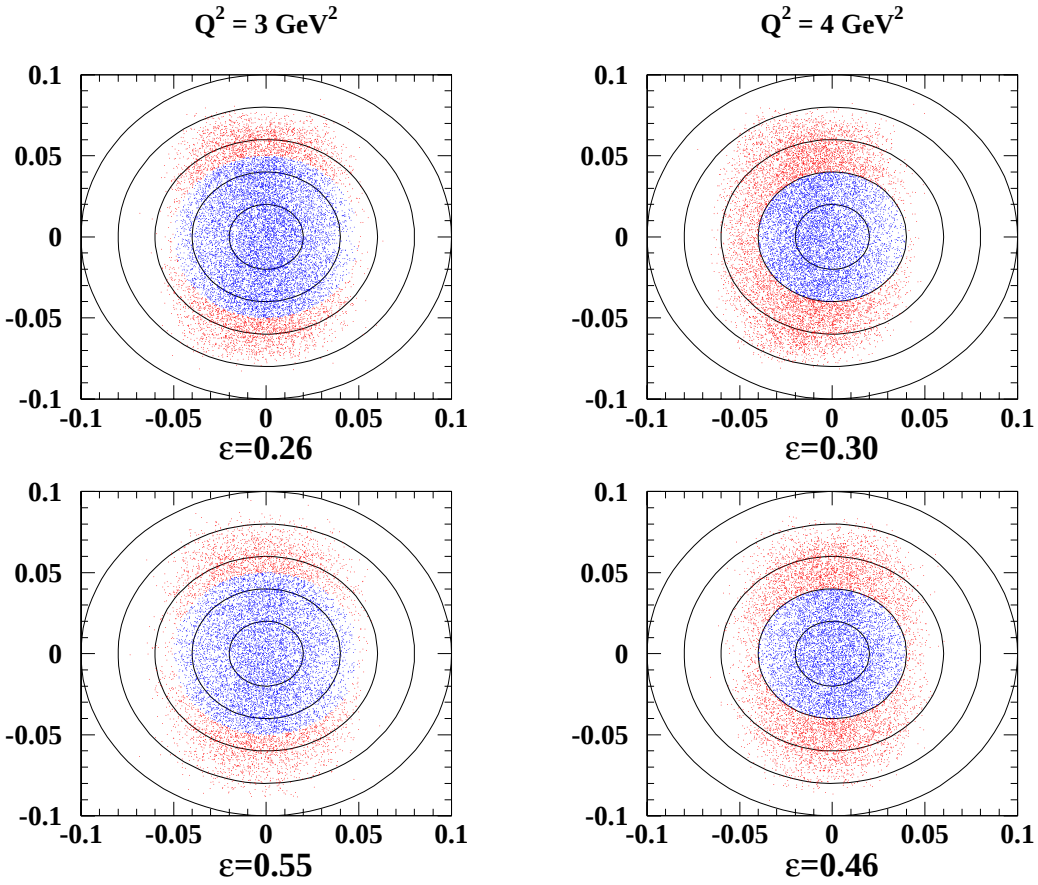

θ_{pq} vs. ϕ_{pq} (polar plot)

Figure 7: Simulated θ_{pq} vs. ϕ_{pq} distributions (polar plots with θ_{pq} the radius) for the $Q^2 = 3.0$ and $Q^2 = 4.0$ GeV^2 kinematics. The top plot for each Q^2 is the low ϵ setting and the bottom plot is the high ϵ setting. The inner, blue region denotes the "complete ϕ_{pq} coverage" region that will be used to extract σ_L. The distribution in the $Q^2 = 4.0$ GeV^2 top plot is somewhat off–center because the HMS cannot quite reach the angle of the direction of **q**. While this requires us to cut away a bit more data, it is necessary to maximize the ϵ range for these kinematics.

Table 5: Projected singles and accidental coincidence rates assuming a 3 cm liquid hydrogen target and 75 μA beam. The accidental coincidence rate is calculated assuming a 2 ns coincidence–time window, 1000:1 pion rejection in the SOS, and 50:1 proton rejection in the HMS. Accidental coincidences, when compared to the projected rate of real coincidences, should not be a significant source of background.

ϵ	SOS e^- rate Hz	SOS π^- rate Hz	HMS π^+ rate Hz	HMS proton rate Hz	R_{acc} Hz	R_{real} Hz	R_{real}/R_{acc}
$Q^2 = 3.0$ GeV^2							
0.547	788	19.7 k	2.5 k	1.6 k	0.0041	0.099	24
0.262	114	28.4 k	1.6 k	890	0.0005	0.032	63
$Q^2 = 3.5$ GeV^2							
0.502	550	1.8 k	3.6 k	2.5 k	0.0040	0.085	21
0.294	131	17.6 k	4.0 k	2.0 k	0.0012	0.035	29
$Q^2 = 4.0$ GeV^2							
0.459	385	1.7 k	9.7 k	7.2 k	0.0076	0.050	6.5
0.300	126	4.5 k	23.7 k	11.5 k	0.0062	0.023	3.8

Lightbody and O'Connell [15] while negatively charged pion rates are estimated using a parameterization of SLAC data [16]. Assuming the combination of the SOS gas Cerenkov and shower counter to have a pion rejection factor of 1000:1, pions should have a negligible contribution to accidental coincidences. Positive hadron rates were estimated using a parameterization of bremsstrahlung data in the 5–19 GeV range [17]. In both arms, the total singles rates are well below the several–hundred kHz that each arm can handle. Assuming a proton rejection factor of 50:1 for the HMS aerogel and a pion rejection factor of 1000:1 in the SOS, the total rate of accidental coincidences in a 2 ns window should be,

$$R_{acc} = (R_e + R_{\pi^-}/1000) \times (R_{\pi^+} + R_p/50) \times 2\ 10^{-9}.$$

The accidental coincidence rates, as well as the projected real coincidence rates, are shown in Table 5. Clearly, accidental coincidences should be a small background.

2.4.3 Target Wall Subtraction

Typically, background from the aluminum walls of the cryogenic target is measured using a "dummy" aluminum target. This target consists of two slabs of aluminum separated by the cryogenic target length (in this case 3 cm). The dummy target is 10 times thicker than the target cell walls, allowing one to make the background measurement faster. The maximum current allowed on this target is 30 μA, so the dummy data should come in a factor of 4 (= 10×30 μA/75 μA) faster.

The uncertainty on the total, aluminum–wall–subtracted yield is given by,

$$\frac{\Delta Y}{Y} = \frac{\sqrt{\left(\frac{\Delta Y_{tar}}{Y_{tar}}\right)^2 + x^2\left(\frac{\Delta Y_{dummy}}{Y_{dummy}}\right)^2}}{1-x},$$

where x is the fraction of the measured yield coming from the cell walls and $\Delta Y_{tar}/Y_{tar}$ and $\Delta Y_{dummy}/Y_{dummy}$ are the fractional uncertainties on the cryogenic target (liquid + cell walls) and the dummy target respectively. Experience from previous pion electroproduction experiments in Hall C (E91003 and E93021) indicates that the aluminum background, after kinematic and missing–mass cuts, is about 1% for a 4 cm hydrogen target (scaled to our 3 cm target length, that increases to about 1.3%). A measurement of the aluminum background to about 20% (*i.e.* 25 counts) would increase the statistical uncertainty of our measurement by less than 0.1%. Assuming an $\approx$ 1% aluminum cell wall contribution, we can project the dummy rate:

$$R_{dummy} = 0.01 \times R_{target} \times 4,$$

where the factor of 4 comes from the fact that the dummy data should come in 4 times faster than the cell wall data. The time needed to achieve 20 dummy counts is then,

$$t_{dummy} = 20/R_{dummy} \approx 500/R_{target}.$$

The estimated dummy–running time calculated using the above equation is given in Table 6. We also include an equal amount of time for π^- dummy running. The contribution from the target cell walls will certainly increase in the deuterium data due to the wider missing–mass cut that must be used. However, the dummy yield will also increase due to the wider missing–mass cut. Furthermore, since the deuterium data will be only $\approx$ 500 counts, the potential increase in statistical uncertainty due to increased aluminum backgrounds should not be significant.

Table 6: Time at each setting for aluminum background data–taking. The time given is to accumulate 20% statistical uncertainty on a subtraction of the order 1% (for π^+ on hydrogen). An equivalent amount of time is allocated for π^- running.

Setting	Q^2 (GeV^2)	t_{dummy} $(\pi^+ + \pi^-)$ (hours)
1a	3.0	2.8
1b		8.8
2a	3.5	3.3
2b		7.9
3a	4.0	5.6
3b		11.9
Total		40.3

2.5 Error Estimates

The ratio of longitudinal to transverse cross sections, R, is a critical parameter in an estimate of the error on the longitudinal cross section. For the proposed kinematics, R is fortunately believed to be quite large ($\simeq 3$) as shown in Figure 8.

Previous experience from E93-021, the F_π experiment, suggests that errors of approximately 3% can be maintained for the unseparated $p(e, e'\pi^+)n$ cross section. The error on the acceptance is dominant. However, by reducing the standard LH_2 target cell length from 4 cm to 3 cm, we expect to reduce the uncorrelated error on the acceptance. As shown in Table 7, the total uncorrelated error is expected to be approximately 2% for the π^+ hydrogen data, which is the value we use in our error estimates.

We need to first estimate the error on σ_L. Two measurements at fixed (Q^2 , x_B) and different values of ϵ are needed in order to determine σ_L. Thus if $\sigma_1 = \sigma_T + \epsilon_1\sigma_L$ and $\sigma_2 = \sigma_T + \epsilon_2\sigma_L$ then

$$\sigma_L = \frac{1}{\epsilon_1 - \epsilon_2}(\sigma_1 - \sigma_2).$$

Assuming uncorrelated errors in the measurement of σ_1 and σ_2, we obtain the intermediate expression

$$\frac{\Delta\sigma_L}{\sigma_L} = \frac{1}{(\epsilon_1 - \epsilon_2)}\frac{1}{\sigma_L}\sqrt{\Delta\sigma_1^2 + \Delta\sigma_2^2}.$$

Table 7: Anticipated errors based on E93-021 experience and improvements expected from the use of a shorter (3 cm versus 4 cm) LH_2 target. The uncorrelated errors between the low and high ϵ settings are given in the last column. The numbers in square brackets are the errors for lowest Q^2 point and the numbers in parentheses denote the uncertainties on the π^- cross sections (where different). The uncorrelated errors dominate the final error on σ_L and σ_T.

Source	Error on Cross Section (%)	Uncorrelated Error on Cross Section (%)
Acceptance	2.	1.
Counting Statistics	0.	1. [1.41] (6.4)
Kinematics	1.	1.
Target Density	1.	0.5
Radiative Corrections	1.	0.5
Charge	0.5	0.5
Tracking	0.5	0.25
Coincidence Blocking	0.5	0.0
Cut Dependence	0.5	0.25
π Decay	0.5	0.0
π Absorption	0.5	0.0
Background subtraction	0.25	0.25
Monte Carlo Generator	0.25	0.25
Quadrature Sum	3.1	2.0 [2.23] (6.6)

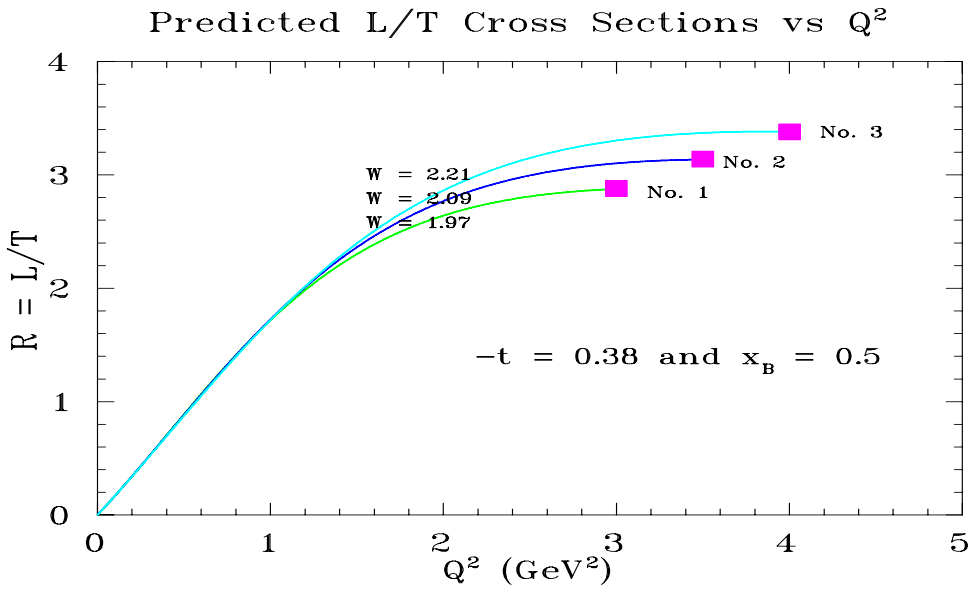

Figure 8: VGL Regge model L/T ratio versus Q^2 for loci of constant W. The proposed kinematic settings are solid squares labeled by number.

and by defining $R \equiv \sigma_L/\sigma_T$ and $\Delta\sigma/\sigma \equiv \Delta\sigma_i/\sigma_i$ and assuming $\Delta\sigma_1/\sigma_1 = \Delta\sigma_2/\sigma_2$, then

$$\frac{\Delta\sigma_L}{\sigma_L} = \frac{1}{\epsilon_1 - \epsilon_2}\frac{\Delta\sigma}{\sigma}\sqrt{(1/R + \epsilon_1)^2 + (1/R + \epsilon_2)^2}$$

This useful equation makes explicit the error amplification due to a limited ϵ range and (potentially) small R. Figure 9 shows the dependence of the relative uncertainty on $\Delta\epsilon$ for three values of σ_L/σ_T. For the proposed experiment, $R \geq 1$, so a limited ϵ lever arm is our primary source of error amplification, a factor of nearly 4 (kinematic settings with larger values of $\Delta\epsilon$ are not possible with the HMS-SOS combination). Given this significant error amplification for uncorrelated errors, we can virtually ignore *correlated* systematic errors of a few percent. The last column of Table 7 lists the uncorrelated errors between the low and high ϵ settings.

2.6 Sensitivity

To demonstrate the potential discrimination power of the experiment, projected errors for the Q^2 dependence of the π^+ longitudinal cross sections are shown in

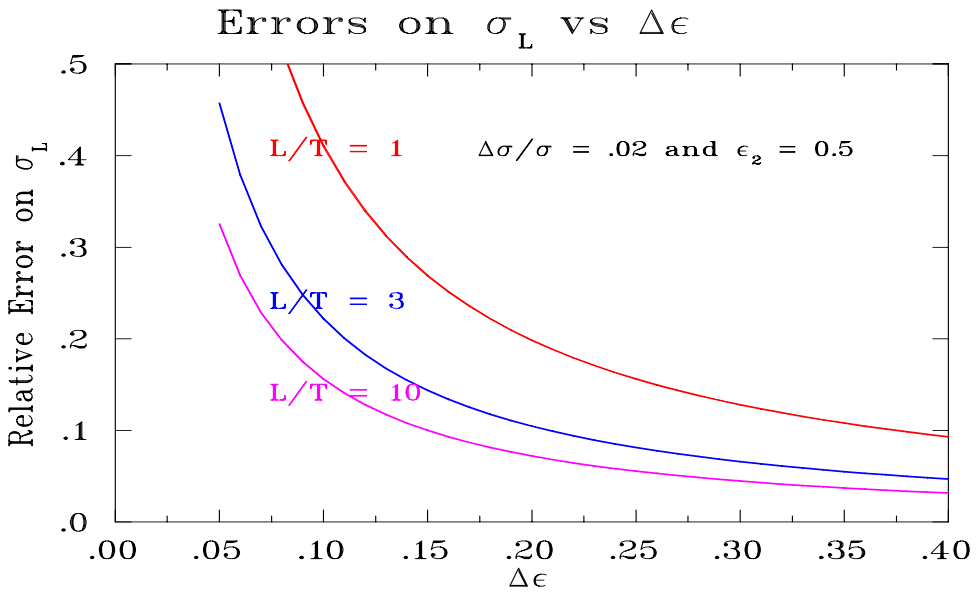

Figure 9: Relative uncertainty of σ_L as a function of $\Delta\epsilon$ for three values of σ_L/σ_T. The important feature to note here is that even when $\Delta\epsilon$ is rather small, one can achieve relatively small uncertainties if σ_L/σ_T is large.

Figure 10. These errors have been estimated using the VGL model for $R = \sigma_L/\sigma_T$ and assuming 2% uncorrrelated errors (except for the lowest Q^2 point). Using only data between $Q^2 = 3$ and 4, the fitted exponent in the Q^2 dependence will be determined at roughly the ± 0.7 level.

Projected uncertainties for σ_T/σ_L for π^- production from the neutron are shown in Fig. 11. The errors are calculated assuming σ_T/σ_L scales as $1/Q^2$ (normalized to one F_π point at $Q^2 = 1.7$ GeV^2) and give an absolute precision of ≈ 0.1. If σ_T/σ_L is significantly larger, the absolute uncertainties on this ratio will also grow, but such a result would mean that that there is a lack of longitudinal dominance and hence no escape from L–T separations in future GPD studies with the π^- reaction.

2.7 Beam Request

Table 8 summarizes our beam request for this experiment. This time will allow us to achieve $\approx 10\%$ errors on measurement of the π^+ longitudinal cross section at three values of Q^2. In addition we will measure σ_T/σ_L for π^- production from the neutron to an absolute precision of 0.1 (assuming the L–to–T ratio is at least 10 to 1). The

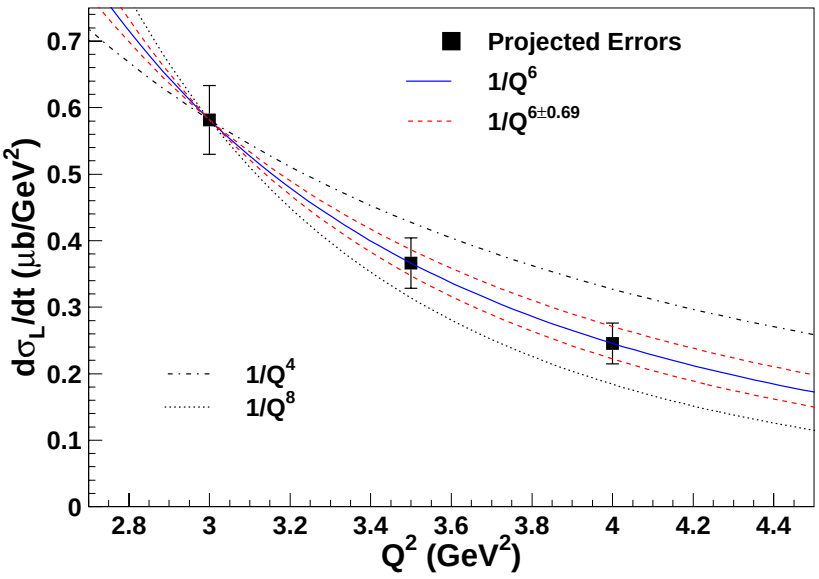

Figure 10: Projected uncertainties for σ_L for π^+ production from the proton. The points are plotted assuming $1/Q^6$ scaling. The uncertainties range from 8.8% at $Q^2 = 3.0$ GeV^2 to 12.6% at $Q^2 = 4.0$ GeV^2. Assuming a form like $1/Q^n$ for the Q^2 dependence of the cross section, we should be able to fit the exponent n to ± 0.69. This is shown by the red, dashed curves. Curves of the form $1/Q^4$ (dashed–dot) and $1/Q^8$ (dotted) are also shown.

beam request includes four hours at each setting for kinematic and target changes (this should be adequate since much configuration can take place during the energy changes required at each point). As written, the kinematics for this experiment will require five different linac energies and three pass changes. We have worked out an alternative plan that would only require four linac energies (and four pass changes), but at the cost of increasing the uncertainties for the Q^2=3.5 Gev^2 longitudinal cross section (from 9.9% to 12.3%). For the purposes of this proposal, we assume the full five linac changes are schedulable, and add an additional three shifts overhead for each linac energy change and one shift for each pass change.

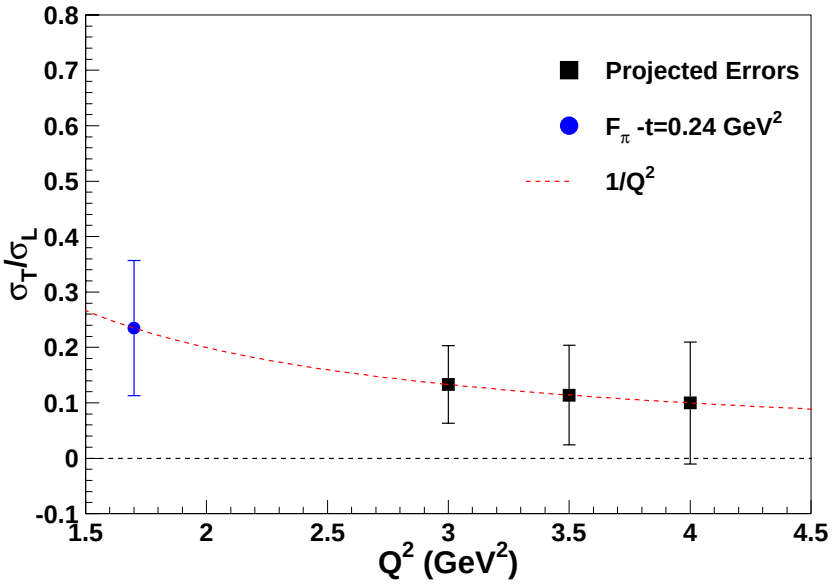

Figure 11: Projected uncertainties for σ_T/σ_L for π^- production from the neutron. In this figure, σ_T/σ_L is assumed to scale like $1/Q^2$ and is normalized to one data point from the F_π experiment at $Q^2 = 1.7$ GeV^2 and $-t = 0.24$ GeV^2. The dashed red line is just the $1/Q^2$ curve.

3 Collaboration

Collaboration members participated in both the F_π and NucPi experiments in Hall C using the same apparatus.

4 Summary

We have proposed a measurement of $p(e, e'\pi^+)n$ at fixed $(-t, x_B)$ in which the contribution due to longitudinal photons will be unambiguously isolated. The momentum transferred by the electron will be as large as $Q^2 = 4$ GeV^2, the highest Q^2 for any L–T separation in pion electroproduction. If charged pion electroproduction at intermediate Q^2 is going to be useful for testing models of polarized GPD's, then

Table 8: Beam request for LH_2 and LD_2 data taking. At each kinematic setting we allow four hours of overhead for kinematic changes (much of the reconfiguration can take place during the energy or pass changes).

Kinematic Setting	Q^2	LH_2 Hours	LD_2 Hours	Dummy Hours	Overhead Hours	Total Hours
1a	3.0	14	4.3	2.8	4	25.1
1b		44	15	8.8	4	71.8
2a	3.5	33	5	3.3	4	45.3
2b		79	12.4	7.9	4	103.3
3a	4.0	56	8.5	5.6	4	74.1
3b		119	19	11.9	4	153.9
5 Energy changes					120	120
3 Pass changes					24	24
$p(e,e'p)$		16				16
Grand Total		361	64.2	40.3	168	633.5 (26.4 days)

we should see evidence for either 1) soft–hard factorization, 2) an approach to it, or 3) a precocious form of soft–hard factorization in the ratios of observables. This experiment will help guide future GPD programs by answering such questions as

• Is $\pi^{\pm}$ electroproduction at intermediate Q^2 close enough to the soft–hard factorization regime that this meson electroproduction reaction can be used to test GPD ansatzes? A restriction to $Q^2 > 4$ would severely limit the phase space of a potential meson electroproduction GPD program at 12 GeV, and might practically limit such studies to high luminosity, small acceptance apparatus.

• Is $R = \sigma_L/\sigma_T$ so large for the π^- channel at high Q^2 that L–T separations won't be needed? This would greatly facilitate a CLAS program of charged pion electroproduction for GPD studies.

5 Acknowledgments

We would like to thank M. Guidal for the version of the VGL computer program used for the rate estimates in this proposal, as well as for many helpful comments on an early draft. Henk Blok and John Arrington also provided many useful comments.

References

[1] J. C. Collins, L. Frankfurt and M. Strikman, Phys. Rev. D **56**, 2982 (1997).

[2] A. Radyushkin, private communication.

[3] M. Vanderhaeghen *et al.*, PRD **60** 094017 (1999).

[4] J. Volmer *et al.*, Phys. Rev. Lett. **86**, 1713 (2001).

[5] L. Mankiewicz, G. Piller and A. Radyushkin, Eur. Phys. J. C **10**, 307 (1999).

[6] J. Volmer, "The Pion Charge Form Factor via Pion Electroproduction on the Proton," Ph.D. Thesis, Vrije Universiteit, 2000.

[7] D. Gaskell, "Longitudinal Electroproduction of Charged Pions from Hydrogen, Deuterium, and Helium–3," Ph.D. Thesis, Oregon State University, 2001.

[8] "The Science Driving the 12 GeV Upgrade of CEBAF," February, 2001.

[9] K. Goeke, . V. Polyakov and M. Vanderhaeghen, Prog. Part. Nucl. Phys. **47**, 401 (2001).

[10] L. L. Frankfurt, P. V. Pobylitsa, . V. Polyakov and M. Strikman, Phys. Rev. D **60**, 014010 (1999).

[11] A. V. Belitsky and D. Muller, Phys. Lett. B **513**, 349 (2001)

[12] V. Tadevosyan for the F_π Collaboration, private communication.

[13] M. Vanderhaeghen, M. Guidal and J. M. Laget, Phys. Rev. C **57**, 1454 (1998).

[14] R. Mohring, "A Comparison of Longitudinal and Transverse Cross Sections in the p(e,e'K^+)Λ and p(e,e'K^+)Σ^0 Reactions," Ph.D. Thesis, University of Maryland, 1999.

[15] J. O'Connell and J. Lightbody, Comp. in Phys., May–June **57** (1998).

[16] J. Arrington, private communication.

[17] R. Ent, private communication.